Journal of Catalysis **196,** 287–292 (2000)
doi:10.1006/jcat.2000.3051, available online at http://www.idealibrary.com on IDEAL®

Direct Oxidation of Methane to Methanol by Mercuric Sulfate Catalyst

Xiao Gang, Henning Birch, Yimin Zhu, Hans Aage Hjuler, and Niels J. Bjerrum[1]

Department of Chemistry, Technical University of Denmark, Building 207, DK-2800 Lyngby, Denmark

Received March 24, 2000; revised August 21, 2000; accepted August 28, 2000

A mercury-catalyzed system using H_2SO_4–SO_3 as the reaction medium for the oxidation of methane to methanol has been studied in the temperature range 150–200°C at methane pressure from 40 bar to 100 bar. Systematic experimental designs were applied to study the effect of temperature, gas pressure, catalyst amount, reaction rate, and liquid agitation speed. The experiments were performed in a high-pressure reactor. The system for the catalytic conversion of methane to methanol using $HgSO_4$ as catalyst is a very efficient process. Analyzing the pressure–time relationship of the reaction gives well-defined information about the reaction rate and indicates a one-to-one reaction between $HgSO_4$ and methane. The pressure drops after the reaction equilibrium is reached are the same independent of catalyst amount. Higher reaction temperature and pressure lead to higher reaction rate. The effect of adding $HgSO_4$ stops when the solubility of $HgSO_4$ in the reaction media is reached.

Key Words: **catalyst; conversion of methane; $HgSO_4$; SO_3; H_2SO_4.**

INTRODUCTION

Methane is a raw material of great synthetic importance and an abundant natural resource as the main constituent of natural gas. Nevertheless, it is often difficult to use because transportation of methane gas or even liquefied natural gas is expensive. Further, methane is a very stable molecule and its direct conversion to useful chemicals is very difficult. It has often been suggested that natural gas should be converted to more easily transported liquid fuel.

The conversion of natural gas into liquid products (1) such as methanol has been practiced for years via steam re-forming and partial oxidation followed by syngas conversion (2). The endothermicity results from addition of steam in which a significant amount of energy is required to decompose water into its elements. Thus such technology based on the high-temperature, energy-intensive conversion of methane and water to carbon monoxide and hydrogen and back to methanol is uneconomical.

[1] To whom correspondence should be addressed. Fax: +45 45 88 31 36. E-mail: njb@kemi.dtu.dk.

Some efforts have been directed at replacing the current capital intensive methane-to-methanol technology based on syngas with a more efficient, direct oxidation process that is less capital intensive. Among most of the attempts only low yields (∼2%) have been reported (3–6). However, one particular high-yield system for the catalytic conversion of methane to methanol was published in 1992 (7). In this system a homogeneous reaction takes place in concentrated sulfuric acid and is catalyzed by mercuric sulfate, $HgSO_4$. The desired intermediate reaction product is methyl bisulfate (CH_3OSO_3H), which is separately hydrolyzed to methanol:

$$CH_4 + 2H_2SO_4 \rightarrow CH_3OSO_3H + 2H_2O + SO_2 \quad [1]$$

$$CH_3OSO_3H + H_2O \rightarrow CH_3OH + H_2SO_4. \quad [2]$$

Sulfuric acid has several roles in this process. First, it is a strong acid giving a superacidic function to the Hg(II)-catalyzed system. Second, sulfuric acid acts as an oxygen transfer agent being itself reduced to sulfur dioxide. Further, it is a reactant to be combined with methane and also a solvent for methane and the reaction products.

The activation of methane is believed to occur through an electrophilic displacement reaction with methyl mercuric bisulfate CH_3HgOSO_3H as an intermediate product. This species decomposes readily to methyl bisulfate and mercurous bisulfate, which is further oxidized to mercuric bisulfate by sulfuric acid to complete the catalytic cycle (8).

Recently platinum catalysts have been reported for the direct, low-temperature, oxidative conversion of methane to a methanol derivative using the same reaction concept as with $HgSO_4$ (9).

In the present work, the homogeneous reaction system using $HgSO_4$ is studied in more detail. Systematic experimental design is applied to study the gas pressure–reaction time relationship at different $HgSO_4$ concentrations, and the reaction rate (pressure slope, bar/s)–$HgSO_4$ concentration relationship at different temperatures and pressures. The impeller geometry is defined, and the gas pressure–rotation speed relationship as well as the reaction rate (pressure slope, bar/s) relationship are investigated.

0021-9517/00 $35.00

EXPERIMENTAL

The Reactor

A high-pressure autoclave reactor (Fig. 1) constructed in this laboratory was used in the experiments. The total internal volume of the reactor was 200 ml. A glass liner was placed inside the reactor to separate the catalyst and reaction liquid from the reactor wall. A vacuum- and pressure-tight magnetic stirrer was fixed through the reactor lid to agitate the reaction mixture. The reactor was heated on the outer wall and the temperature was controlled using a PID temperature controller. An electronic pressure sensor (WIKA Tronic line Transmitter 891.23.510, WIKA Alexander Wiegand GmbH & Co.) was connected to measure the gas pressure inside the reactor. In order to examine the reaction mechanisms it was necessary to run the reaction with a well-defined reaction time. This was obtained by heating the reactor content to the desired temperature before introducing methane into the reactor. To minimize the drastic temperature decrease of the reactants caused by introduction of cold methane, a heating system (preheater) was designed to preheat methane to the reaction temperature before its introduction into the reactor.

Chemicals

Oleum, 65% SO_3, Merck.
$HgSO_4$, assay min. 99%, Riedel-de Haën.
CH_4, N25, Hede Nielsen A/S.

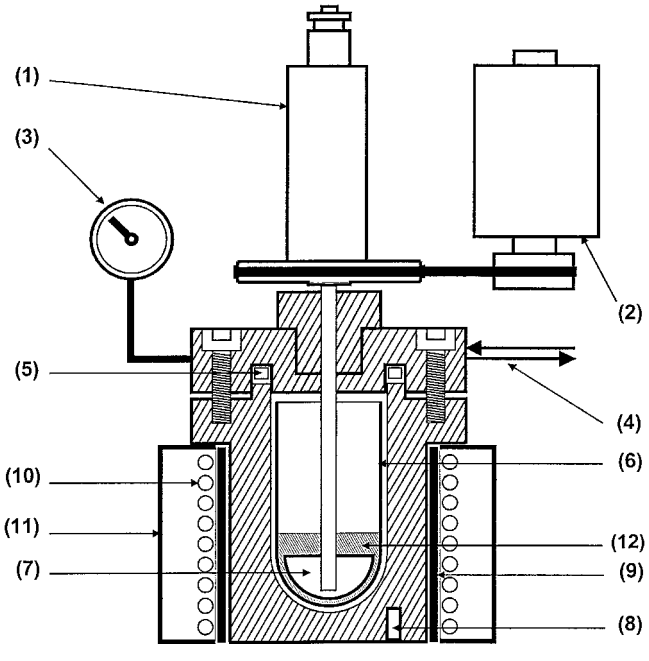

FIG. 1. Schematic drawing of the reactor: (1) magnetic stirrer; (2) electric motor; (3) pressure unit; (4) gas inlet/outlet; (5) PTFE gasket; (6) glass liner; (7) impeller; (8) thermocouple; (9) heating element; (10) cooling tube; (11) isolator; (12) reaction media.

The Gas Chromatograph (GC)

A gas chromatograph (Hewlett Packard 6890) equipped with a thermal conductivity detector was used to measure the gas compositions in the reactor before and after the reactions. Gas sampling bags were used to collect the gas from the reactor. Helium was used as the carrier gas. The column was of the type HP-PLOT Q (divinylbenzene/styrene polymer).

The High-Performance Liquid Chromatograph (HPLC)

A high-performance liquid chromatograph (Shimadzu SCL-10Avp) was used to measure the methanol produced during the reactions. The system consists of a high-pressure pump (LC-10AD), a column (Nucleosil 100-5 C18), a column oven (CTO-10Asvp), and a refractive index detector (Shimadzu RID 10A).

The catalysts and the oleum (H_2SO_4–SO_3) were added to the reactor. The reactor was closed and heated to the reaction temperature. The reactor was thereafter pressured with preheated methane to the desired pressure. The contents of the reactor were stirred with an impeller placed on the magnetic stirrer at a chosen rotation speed. After a certain reaction time, the stirring was stopped and the reactor was cooled to room temperature. The gas mixture in the reactor was collected for gas chromatographic analysis. The liquid content in the reactor was transferred to a glass bottle. An aliquot of the liquid was diluted 20 times with distilled water and the resulting solution was hydrolyzed in a sealed container for 3 h at 100°C. The resulting solution was quantitatively analyzed for free methanol by high-performance liquid chromatography. All experiments were done under comprehensive safety precautions.

RESULTS AND DISCUSSION

Figure 2 shows a typical plot of reactor pressure vs reaction time. It is seen that, at the starting stage, the pressure of SO_3 (from 65 wt% oleum) increases with increasing temperature (A). After the reactor is pressurized with CH_4 and the stirring is started, the pressure starts dropping (E) because the reactant CH_4 is consumed and the product SO_2 is partly dissolved in the oleum as reaction (1) proceeds. After a certain time the reaction equilibrium is reached and the pressure curve starts flattening (F). The experiment is terminated by stopping the heating and agitation, and cooling the reactor with cooling water (G).

The above-mentioned procedure was applied to investigate the gas pressure–reaction time relationship at different $HgSO_4$ concentrations (Fig. 3). The $HgSO_4$ concentration is defined as the weight percent of $HgSO_4$ in the reaction liquid. From Fig. 3 and Table 1 it can be seen that curves A, B, and C, corresponding to 1.00 wt%, 0.40 wt%, and 0.10 wt% of $HgSO_4$, respectively, after their equilibrium states are

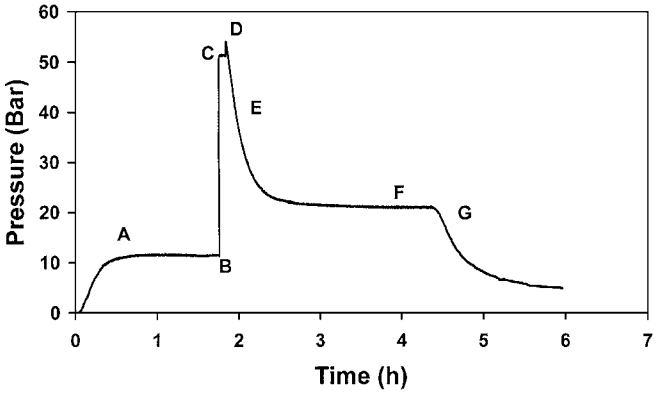

FIG. 2. Plot of reactor pressure vs reaction time: (A) heating of the H_2SO_4; (B) introduction of the preheated CH_4; (C) desired pressure is reached; (D) stirrer started; (E) pressure drop due to the reaction; (F) reaction has reached equilibrium; (G) heating and stirring stopped, water-cooling started.

reached, have approximately the same pressure drop (ΔP) and the CH_3OH product concentrations (millimoles per liter) are also almost the same. This phenomenon confirms that $HgSO_4$ is really a catalyst since the reaction equilibrium is independent of the catalyst amount. From the trends of curves A to F in Fig. 3 we can see that, when the other conditions remain the same, increasing the amount of $HgSO_4$ results in a faster reaction rate and therefore a shorter reaction time to reach the reaction equilibrium.

Considering the perspective of applying the reaction to a continuous process where the products are constantly removed from the reactor it is important to find the optimal catalyst concentration corresponding to the fastest reaction rate. The initial slopes (bar per second) of a pressure–time curve (such as in Fig. 3) are proportional to the reaction rate (under the assumption that the equilibrium conditions are

TABLE 1

Selected Experimental Results from Fig. 3

Test no.	$HgSO_4$ (wt%)	ΔP (bar)	CH_3OH (mmol/l)	Pressure slope (bar/s) $\times 10^{-2}$
A	1.00	32	94	7.19
B	0.40	31	92	3.26
C	0.10	31	97	0.74

independent of the $HgSO_4$ concentration). Figure 4 shows a plot of initial pressure slope vs $HgSO_4$ concentration at different reaction temperatures. For example, when the reaction temperature is 180°C, the pressure slope increases approximately linearly with increasing $HgSO_4$ concentration until it reaches ca. 0.03 bar/s corresponding to a $HgSO_4$ concentration of ca. 0.8 wt%. After this point the pressure slope remains approximately at the same value even though the $HgSO_4$ concentration is increased. This phenomenon indicates that it is the solubility of $HgSO_4$ in concentrated H_2SO_4 that dominates the reaction rate. That is to say that 65 wt% oleum can only dissolve up to ca. 0.8 wt% of $HgSO_4$ at the selected temperature (and solvent conditions). More than 0.8 wt% of $HgSO_4$ will not contribute to a faster reaction rate. The same trend is also true for the other two curves in Fig. 4, namely, when reaction temperatures are 150°C and 200°C, respectively. Lower reaction temperatures (e.g., 150°C) result in lower reaction rates, and higher reaction temperatures (e.g., 200°C) result in higher reaction rates. The pressure slopes are calculated by a linear regression of the pressure drop (bar) vs reaction time (seconds). The time scale for the linear regression is from the 100th second to the 200th second after stirring starts (D in Fig. 2). The absolute values of the slopes are used. It is also seen that the solubility of $HgSO_4$ in oleum is different in these three cases. It is interesting to note that, among these three

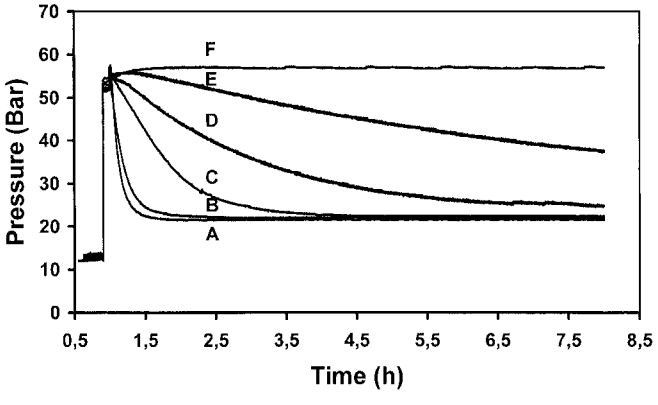

FIG. 3. Plot of pressure vs reaction time with different $HgSO_4$ concentrations: (A) 1.00 wt% $HgSO_4$, (B) 0.40 wt% $HgSO_4$, (C) 0.10 wt% $HgSO_4$, (D) 0.04 wt% $HgSO_4$, (E) 0.008 wt% $HgSO_4$, (F) 0 wt% $HgSO_4$. Temperature, 180°C; 50 ml of 65 wt% oleum; agitation speed, 850 rpm.

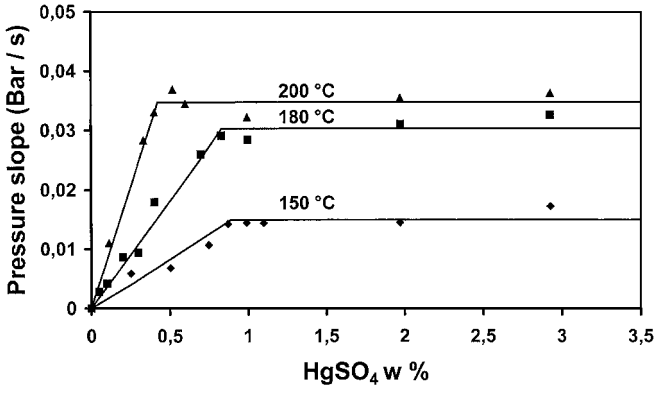

FIG. 4. Plot of pressure slope vs $HgSO_4$ concentration at different temperatures. Pressure, 50 bar; 50 ml of 65 wt% oleum; agitation speed, 550 rpm.

curves, the highest reaction temperature (i.e., 200°C) results in the lowest $HgSO_4$ solubility (ca. 0.42 wt%), and the lowest reaction temperature results in highest $HgSO_4$ solubility (ca. 0.87 wt%). Normally one would expect that higher temperature results in higher solubility and vice versa. But apparently that is not the case here. This is believed to be related to the solubility of SO_3 in oleum. Regarding to the solubility of $HgSO_4$ in oleum we assume the following equations to apply,

$$[Hg^{2+}][SO_4^{2-}] = K \quad [3]$$

$$SO_4^{2-} + SO_3 \leftrightharpoons S_2O_7^{2-}, \quad [4]$$

where K is the solubility product. Our reactor is built in such a way that the gas-phase volume is rather large compared to the liquid-phase volume. At higher temperatures (i.e., 200°C) a substantial part of the dissolved SO_3 is evaporated into the gas phase resulting in lower SO_3 concentration in the liquid phase. This fact leads to a decrement of the SO_3 concentration resulting in an increment of the SO_4^{2-} concentration (according to Eq. [4]) and again to a decrement of Hg^{2+} concentration according to Eq. [3].

Figure 5 shows the plot of initial pressure slope vs $HgSO_4$ concentration at 180°C and different gas pressures. These curves are similar to those in Fig. 4 in the respect that a concentration value for $HgSO_4$ can be found in each curve at which a higher concentration will not lead to higher reaction rates. At any given $HgSO_4$ concentration the pressure slope (reaction rate) is higher with higher gas pressure and lower with lower gas pressure.

Computer modeling was applied to analyze the reaction rate. Figure 6 shows the pressure–time relationship at different $HgSO_4$ concentrations. The mathematical model found to best fit the curves is

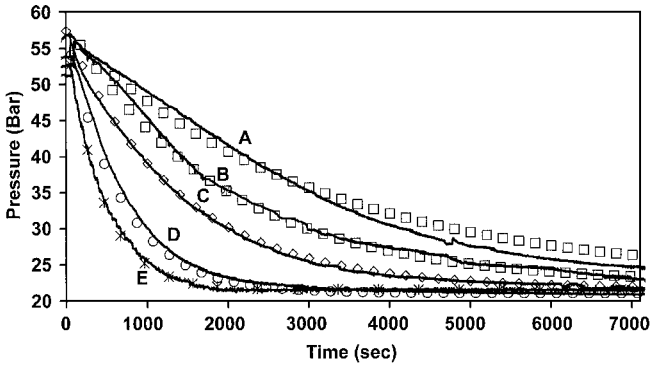

FIG. 6. Computer modeling of pressure–time relationship. $HgSO_4$ concentration: (A) 6.7 mmol/l; (B) 10.0 mmol/l; (C) 13.4 mmol/l; (D) 26.8 mmol/l; (E) 46.9 mmol/l. The reaction time is counted from the agitation starting point.

$$P = P_o - P_e\, e^{-k(t-t_o)} + P_e, \quad [5]$$

where P is the pressure of the gas mixture at time t, P_o is the initial pressure, P_e is the pressure when the reaction reaches the equilibrium state, t_o is the time when the reaction starts, and k is a constant describing the pressure dropping rate against reaction time. From Fig. 6 it can be seen that the mathematical modeling (marked points) fit the original data (the continuous curves) very well, indicating that we are dealing with a first-order reaction.

From Eq. [3] we can get

$$\ln(P - P_e) = \ln(P_o - P_e) - k(t - t_o). \quad [6]$$

The plot of $\ln(P - P_e)$ vs t is shown in Fig. 7 where straight lines are obtained. The slopes of the straight lines are the k values for the respective reactions. Plotting the relationship

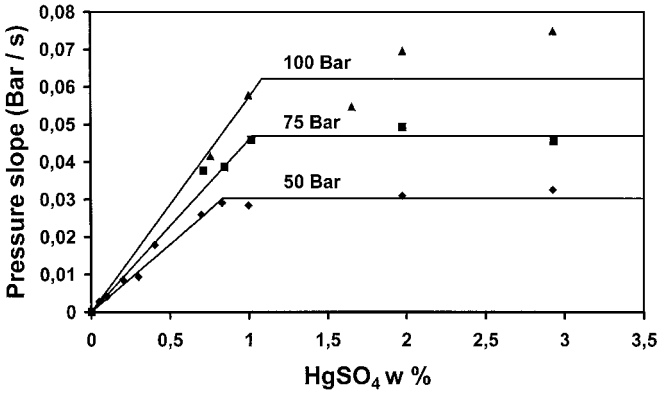

FIG. 5. Plot of pressure slope vs $HgSO_4$ concentration at different pressures. Temperature, 180°C; 50 ml of 65 wt% oleum; agitation speed, 550 rpm.

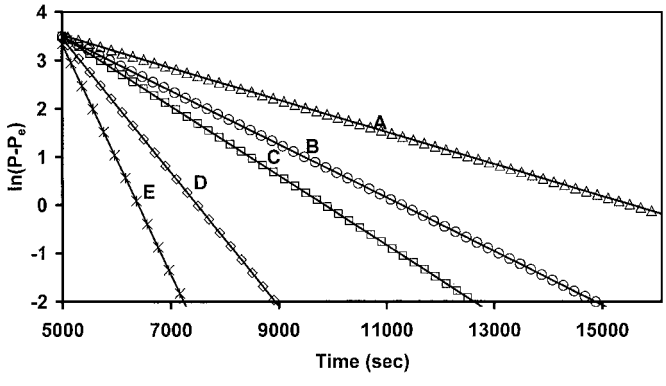

FIG. 7. Plot of $\ln(P - P_e)$ vs time. $HgSO_4$ concentration: (A) 6.7 mmol/l; (B) 10.0 mmol/l; (C) 13.4 mmol/l; (D) 26.8 mmol/l; (E) 46.9 mmol/l.

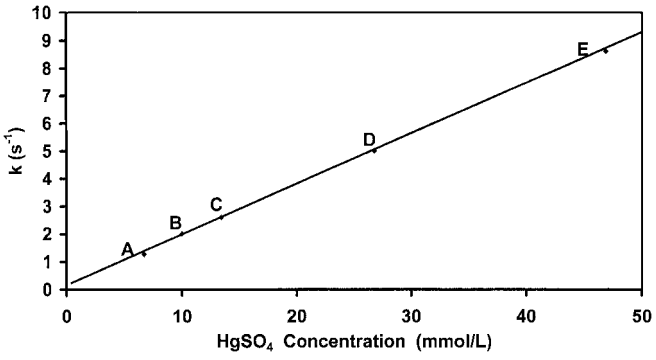

FIG. 8. Plot of pressure dropping rate k vs $HgSO_4$ concentration. $HgSO_4$ concentration: (A) 6.7 mmol/l; (B) 10.0 mmol/l; (C) 13.4 mmol/l; (D) 26.8 mmol/l; (E) 46.9 mmol/l.

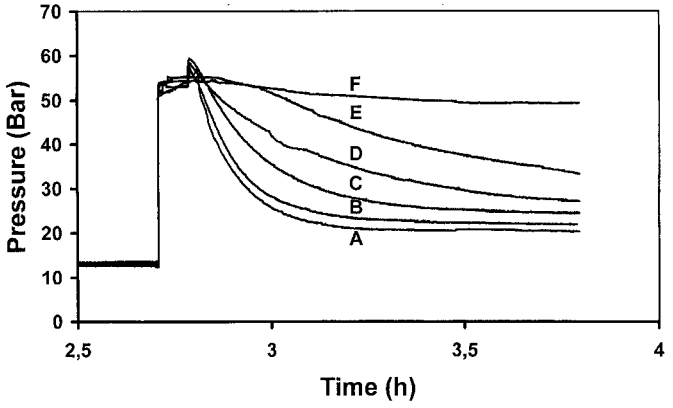

FIG. 10. Plot of pressure vs reaction time at different agitation speeds: (A) 1640 rpm, (B) 850 rpm, (C) 630 rpm, (D) 420 rpm, (E) 200 rpm, (F) 0 rpm.

between k and the $HgSO_4$ concentration (Fig. 8) also gives a straight line with a slope $k_c = 0.18$ l mmol^{-1} s^{-1}. Here $k_c = k/c$ (k_c is defined as the constant describing the relationship between reaction pressure dropping rate and catalyst concentration c). It should be noted that the linearity of the curve in Fig. 8 was expected because the measurements were made corresponding to the first linear part of curve B in Fig. 4. These results indicate that the methane reacts with $HgSO_4$ in a one-to-one reaction which can be expressed by $d(CH_4)/dt = k_1 P_{CH_4}$ [Hg^{2+}], where k_1 is the rate constant of the CH_4–Hg^{2+} reaction, and P_{CH_4} and [Hg^{2+}] are the CH_4 pressure and Hg^{2+} concentration, respectively.

Gas–liquid stirred vessels are widely used in industry as reactors. Mechanical agitation of the reactants plays an important role in mass transfer and reaction rate. We have attempted to characterize the relationship between reaction rate and stirring speed using our laboratory impeller model. Figure 9 shows the geometry and dimension of the impeller (see Fig. 1 for the position of the impeller in the reactor). A plot of pressure vs time with different rotation speeds is shown in Fig. 10. We have varied the rotation speed from 0 to 1600 rpm. Figure 11 shows a plot of pressure slope vs impeller rotation speed. We notice that, even without stirring, the reaction still takes place although at a very low rate (the pressure slope at 0 rotation speed is not 0 but 0.0051 bar/s). It can be seen that the reaction rate increases with increasing rotation speed. This is because the increment of rotation speed will bring more gas in contact with the liquid. However, when the rotation speed is larger than 720 rpm (corresponding to a pressure slope of ca. 0.05 bar/s), the reaction rate does not increase anymore even if rotation speed increases. This is thought to be related to the contact surface area of the liquid and gas phases, where CH_4, oleum, and $HgSO_4$ are present at the same time. The contact surface areas increase with increasing rotation speed, but not

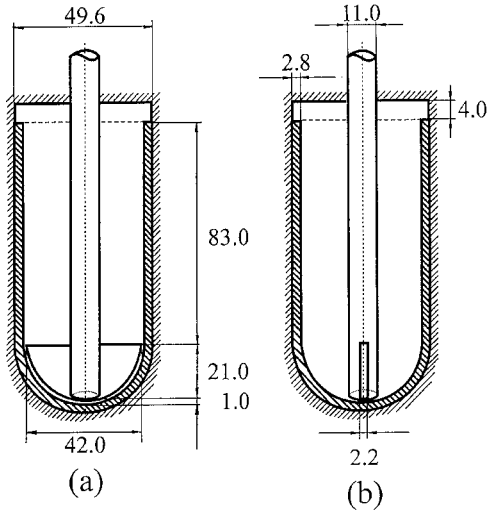

FIG. 9. Drawing and dimensions of the impeller and the glass liner: (a) front view and (b) side view.

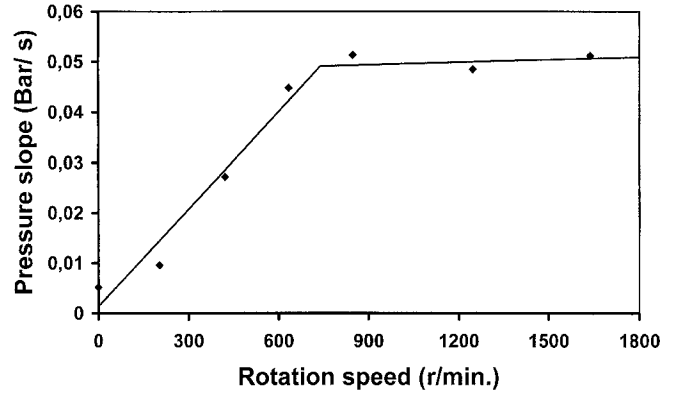

FIG. 11. Plot of pressure slope vs rotation speed. 1.97 % w/w $HgSO_4$; 50 ml of 65 wt% oleum; 180°C.

proportionally all the way. Due to the liquid surface tension and the reactor geometry the contact surface area will stop increasing at a certain rotation speed resulting in the relatively unchanged pressure slope in the last part of the curve.

CONCLUSION

The system for the catalytic conversion of methane to methanol using $HgSO_4$ as catalyst in oleum is a very effective process. Analyses of the pressure–time relationship of the reaction gives well-defined information about the reaction rate and shows that we are dealing with a first-order reaction, where the rate constant is proportional to the $HgSO_4$ concentration. The solubility of $HgSO_4$ in oleum is the limiting factor in the reaction rate. Higher reaction temperatures and pressures lead to higher reaction rates. The impeller rotation speed plays an important role in the reaction rate. To a certain point the reaction rate increases with increasing rotation speed, after which the reaction rate remains constant, probably because the contact surface area between the liquid and the gas phase stops increasing with increasing impeller rotation speed.

ACKNOWLEDGMENTS

This investigation has been supported by the Danish Natural Science Research Council THOR-project no. 9700900.

REFERENCES

1. Mills, G. A., *Fuel* **73**, 1243 (1994).
2. Rostrup-Nielsen, J. R., Dybkjær, I., and Christiansen, L. J., Steam Reforming. Opportunities and Limits of the Technology, *in* "NATO ASI Chemical Reactor Technology for Environmentally Safe Reactors and Products" (H. de Lasa, Ed.), p. 249. Kluwer, Dordrecht, 1992.
3. Hunter, N. R., Gesser, H. D., Morton, L. A., Yarlogadda, P. S., and Fung, D. P. C., *Appl. Catal.* **57**, 45 (1990).
4. "Methane Conversion by Oxidation Processes" (E. E. Wolf, Ed.), p. 403. Van Nostrand Reinhold, New York, 1992.
5. Gesser, H. D., Hunter, N. R., and Prakash, C. B., *Chem. Rev.* **85**, 235 (1985).
6. Foster, N. R., *Appl. Catal.* **19**, 1 (1985).
7. Periana, R. A., Taube, D. J., Taube, H., and Evitt, E. R., International Patent Application W092/14738, 1992.
8. Periana, R. A., Taube, D. J., Evitt, E. R., Löffler, D. G., Wentrcek, P. R., Voss, G., and Masuda, T., *Science* **259**, 340 (1993).
9. Periana, R. A., Taube, D. J., Gamble, S., Taube, H., Satoh, T., and Fujii, H., *Science* **280**, 560 (1998).